

## Modeling the impact of rotor movement on non-linearity of motor currents waveforms in high-speed PMSM drives

Leszek Jarzebowicz<sup>1</sup>, Slobodan Mirchevski<sup>2</sup>

GDANSK UNIVERSITY OF  
TECHNOLOGY

Faculty of Electrical and Control  
Engineering, Narutowicza St. 11/12,  
80-233 Gdansk, Poland

E-mail: [leszek.jarzebowicz@pg.gda.pl](mailto:leszek.jarzebowicz@pg.gda.pl)

URL: <http://www.pg.edu.pl>

SS. CYRIL AND METHODIUS  
UNIVERSITY

Faculty of Electrical Engineering and  
Information Technologies, 1000 Skopje,  
Republic of Macedonia

E-mail: [mirceslo@feit.ukim.edu.mk](mailto:mirceslo@feit.ukim.edu.mk)

URL: <http://en.feit.ukim.edu.mk>

### Keywords

«Electrical drive», «Modelling», «Pulse Width Modulation (PWM)», «High-speed drive», «Traction application»

### Abstract

Motor current measurement techniques as well as predictive control algorithms for electric drives rely on an assumption of linear motor currents changes resulting from constant inverter output voltages. Recent research has reported that this assumption does not hold in motors with short electrical time constant, and in drives whose rotor position advances substantially during a control period. This paper proposes a simulation model that reflects the non-linearity of currents waveforms. The hybrid model, designed in Matlab/Simulink, consists of both continuous- and discrete-time subsystems. Operation of the inverter can be reproduced in either a simplified manner - by reflecting only the fundamental voltage component, or in detail – by modeling the pulse-width-modulated motor voltages. The proposed model is validated with respect to reproducing the non-linearity of currents waveforms by comparison with a laboratory high-speed PMSM drive.

### Introduction

Contemporary electric drives are controlled by microprocessors. The digitally implemented control algorithm computes motor terminal voltages, to be produced by the inverter based on pulse width modulation (PWM) technique. Voltage modulation uses multiple transistors' switching within each control cycle, to match the reference voltage in terms of mean value. This switching produces substantial ripple component superimposed on motor currents (Fig. 1). The ripples are inevitable, but the control algorithm aims at regulating only the fundamental component of motor currents, which is defined as a theoretical response to constant motor voltage over a control cycle, whose value equals to the mean of modulated voltage (voltage fundamental component). Thus, the fundamental current component should be extracted by specific measurement technique in order to provide stable and accurate current control. A solution to this problem, named synchronous sampling, was reported by Matsui *et al.* [1]. The authors stated that instantaneous motor current, when sampled in the middle or at the border of PWM cycle, corresponds to its fundamental component and simultaneously to the mean value over a PWM cycle. This has been proven for symmetrical PWM method by using the assumption that motor currents change in a linear manner during stable inverter states. Superiority of synchronous sampling over low-pass filtering of rippled currents has been demonstrated in [2].

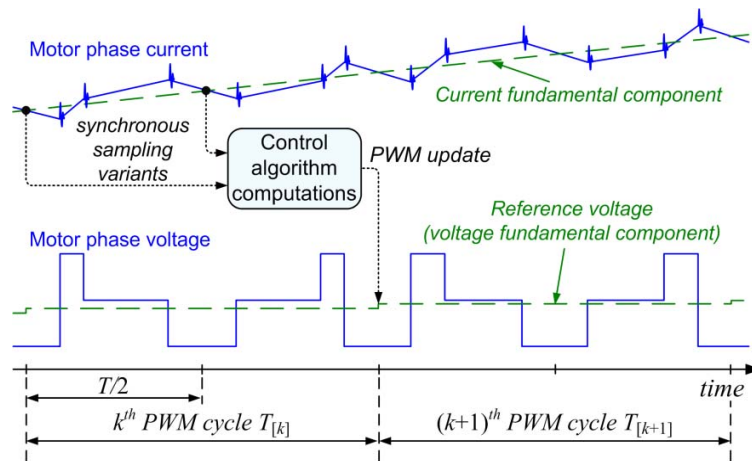


Fig. 1: Waveforms of motor current and voltage in selected phase of a PMSM drive

Whilst synchronous sampling appears to be a well-established approach, some recent papers aim at improving current control dynamics by introducing extraordinary sampling approaches. Böcker and Buchholz [3] have proved that sampling motor currents and updating the PWM generator multiple times within a PWM cycle may significantly improve the control bandwidth. Moreover, increased research focuses on predictive control where forecasting future behavior of the system is based on its model and on a set of possible actuations [4]. Typically, the time horizon for the prediction covers a few control cycles yet some papers have demonstrated that even predicting the current value for the end of the present control cycle contributes to substantial improvement of control dynamics both in PMSM [5] and dc drives [6].

The research reviewed above assumes linear changes of currents resulting from constant voltages at motor terminals. In contrast, Wolf *et al.* [7] have quantified errors of synchronously sampled motor currents, which result from non-linear current changes. The authors indicated that stator resistance should not always be neglected in the motor model because motor electrical time constant may, in some cases, be considerably close to the PWM cycle duration. This, in turn, results in exponential-approximated changes of motor currents. Analytical analysis, as well as simulation and experimental verification, have been carried out using 3-phase RL load that represents an electric motor.

The non-linear changes of motor phase currents have also been associated with progressive rotor movement which takes place within steady supply voltage intervals [8]. This association gains importance since in numerous applications the maximal speed of electric motors has been substantially increased to improve their power-to-volume and power-to-weight ratios [9][10]. For instance, the maximal speed of permanent motor synchronous motor (PMSM) drive in Toyota Prius reaches 13500 rpm; an induction motor in the electric Tesla S revolves up to 16000 rpm. A similar problem appears in high power applications, where rotational speeds are not that high, but the control period, related to the PWM frequency, is kept at a level of a few hundreds of hertz. Consequently, the rotor position may advance up to  $40^\circ$  during a control period if voltage modulation is applied [11] or even by  $60^\circ$  in case of six-step inverter control mode [12].

As the non-linear current changes influence drive's control properties, they should be included in current measurement and prediction techniques. However, a detailed mathematical description of motor phase currents reflecting the non-linear changes is complex and involves continuous input variables, which are not available in microprocessor implementation. Thus, practical approach to this problem should be preceded with numerous model simplifications that will enable the digital execution. Selection of these simplifications should be analyzed based on a reference model, which precisely reflects the considered electro-mechanical dependencies. This paper proposes such a reference model developed in Matlab/Simulink. The focus is pointed at the impact of rotor movement on currents waveforms, but the model does not neglect the stator resistances, hence the non-linearity related to short electrical time constant is also included.

## The modeled relation between rotor movement and currents waveform

The impact of motor speed on the curvature of motor phase currents is hereby explained on an example of non-salient PMSM drive; however, in general this problem concerns also salient motors. Principal relations between instantaneous motor voltages and currents in the stationary 3-phase reference frame are described by the following equation [13]:

$$\begin{bmatrix} u_a \\ u_b \\ u_c \end{bmatrix} = R_s \begin{bmatrix} i_a \\ i_b \\ i_c \end{bmatrix} + \frac{d}{dt} \begin{bmatrix} L_a & M_{ab} & M_{ac} \\ M_{ba} & L_b & M_{bc} \\ M_{ca} & M_{cb} & L_c \end{bmatrix} \begin{bmatrix} i_a \\ i_b \\ i_c \end{bmatrix} + \frac{d}{dt} \begin{bmatrix} \psi_f \cos \theta \\ \psi_f \cos(\theta - 2\pi/3) \\ \psi_f \cos(\theta + 2\pi/3) \end{bmatrix} \quad (1)$$

where:  $a, b, c$  – indexes corresponding to motor phases;  $u, i$  – motor phase voltages and currents, respectively;  $L, M$  – stator self- and mutual inductances, respectively;  $\psi_f$  – permanent magnets' flux linkage;  $\theta$  – rotor angular position.

The resistive voltage drop is typically negligible when compared to the other terms in the equation, especially when considering high-speed operation. Using this assumption and applying vector description, (1) can be rewritten in a simpler form:

$$\mathbf{U}[k] = \mathbf{L} \frac{d\mathbf{I}(t)}{dt} + \mathbf{E}(t) \quad (2)$$

According to (2), the motor current changes with a slope depending on constant inductance  $\mathbf{L}$  and on the difference between supplying voltage  $\mathbf{U}[k]$  and the electromotive force  $\mathbf{E}(t)$ . In quasi-steady state operation, when torque and speed are both constant, the electromotive force vector has constant modulus and its angle advances uniformly. The supply voltage vector is controlled to compensate for the electromotive force and to sustain the rotating stator current vector  $\mathbf{I}(t)$ . Nevertheless, the rotor movement is continuous, thus the angle of electromotive force  $\mathbf{E}(t)$  advances smoothly. In contrast, the supplying voltage vector  $\mathbf{U}[k]$  changes discretely. Depending on the kind of analysis, this vector can represent either the fundamental (mean) value from the modulated voltage when focusing on the fundamental current component or the instantaneous voltage during stable inverter state when analyzing PWM transients. As a result of interaction between this continuous rotor movement and discrete voltage changes, the angular displacement between the electromotive force vector  $\mathbf{E}(t)$  and supplying voltage vector  $\mathbf{U}[k]$  varies within the control period. This causes that the voltage drop  $\mathbf{L}(d\mathbf{I}(t)/dt)$  varies and – as the inductance  $\mathbf{L}$  is constant – makes the slope of current  $\mathbf{I}(t)$  change. The mathematical description of this relation is more complex in salient PMSMs, where the inductances  $\mathbf{L}$  are a function of rotor position  $\theta$ .

## The proposed reference model

A hybrid simulation model, consisting of both continuous- and discrete-time subsystems, is proposed to reflect the non-linearity of motor currents waveforms (Fig. 2). The PMSM subsystem is based on the standard equations describing voltages in the  $d$ - $q$  coordinate frame [14]. The subsystem is supplemented with Park and Clark transformations in order to operate with phase-oriented inputs and outputs [15]. The above-described part is modeled in continuous-time to reflect the progressive rotor movement.

The other part of the model, corresponding to the controller and inverter, is modeled in discrete time. A 10-kHz triggering clock provides the discrete subsystems with a square-wave signal whose edges correspond to distinctive control events. The rising edge corresponds to the midpoint of PWM cycle and it triggers the control algorithm computations. Thus, the feedback signals are sampled in the midpoint of PWM and the control algorithm computes the reference voltages based on these samples. The falling edges of the square-wave signal mark the margins of PWM cycles, and they are used to produce the waveforms of inverter output voltages. Operation of the PWM generator and the inverter can be modeled in two variants. The first operating mode reflects only the fundamental voltage and

current components, marked with dashed line in Fig. 1. In this case, the voltages at motor terminals are constant during the control period and equal to the mean of actual modulated voltages. The second operating mode reflects PWM, though the inverter transistors are modeled to have ideal static and dynamic characteristics. Thus, neither current switching disturbances nor voltage drops on power electronic devices are included. The 'Inverter modeling mode' block forwards the clocking signal to a particular voltage computation path, depending on 'Inverter mode' value: 0 – fundamental component; 1 – PWM.

The 'Fundamental component modeling' block includes only the inverse Clarke transformation. As it is executed at the margin of control periods, and its output value is held until between executions. This way the fundamental phase voltage components are produced to feed the motor.

The 'SVM switched-on times computation' block determines the conduction times of the upper transistors in each inverter leg according to [16]. This computation is performed at the beginning of each PWM cycle. Next, the computed times are passed to 'PWM modeling' block (Fig. 3), which uses them to set three comparators. The operation of this block is similar to actual microprocessor, which applies an up-down counter running at a PWM frequency and three comparators to determine the switching instants in particular inverter legs. Depending on the results of the three comparisons, the motor phase voltages are determined with respect to the assumed dc-link voltage.

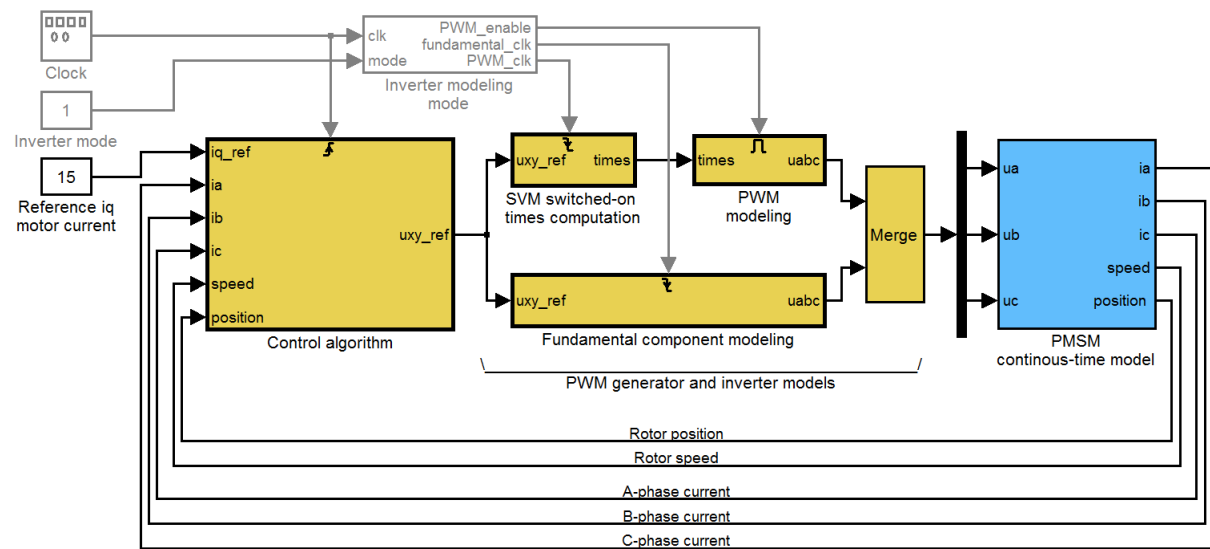


Fig. 2: General structure of the reference model

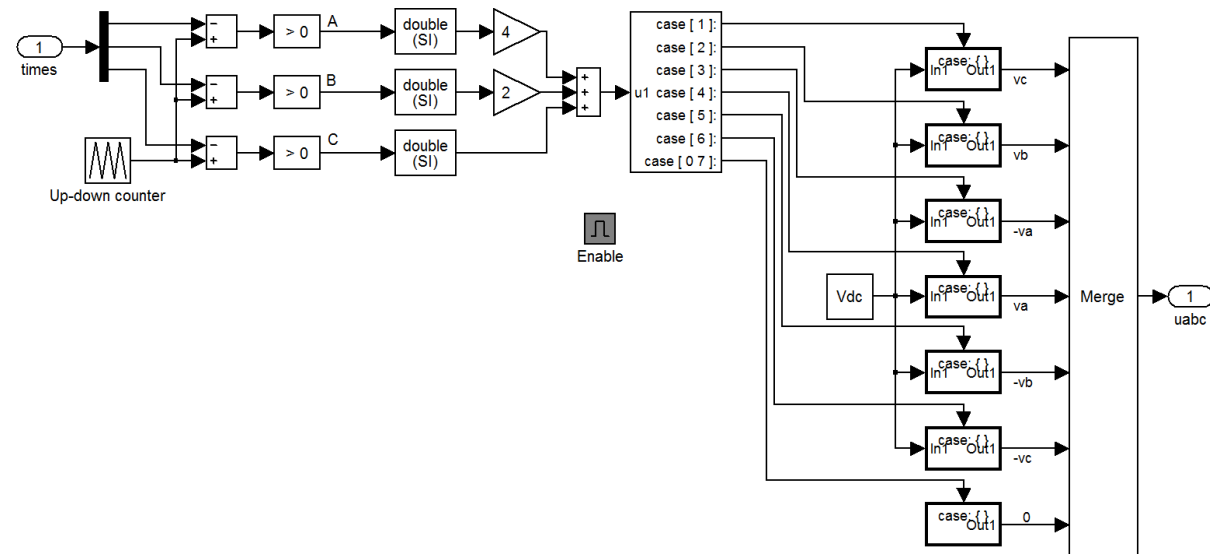


Fig. 3: PWM modeling approach

## Validation

Validation of the reference model aims at verifying if it properly reflects the impact of progressive rotor movement on motor phase currents waveforms. For this purpose, the model was parametrized according to a high-speed laboratory drive, which allowed for comparison between simulation and experimental outcomes. Parameters of the laboratory drive are given in Table I. The drive favors the non-linear current changes related to the progressive rotor movement. For operation at the rated speed  $\omega_{mn}$ , the change in rotor position during the PWM cycle reaches  $\Delta\theta = \omega_{mn}/f = 0.44$  rad, i.e.  $25^\circ$ .

**Table I: Parameters of the laboratory PMSM drive**

Parameter	Value
PWM frequency $f$	5 kHz
Rated speed (electrical) $\omega_h$	2200 rad/s
Rated (r.m.s.) phase current $I_n$	10 A
Stator resistance $R_s$	0.1 $\Omega$
Stator inductance $L_q$	1.0 mH
Flux linkage due to the rotor magnets $\psi_f$	75 mWb
Inverter input voltage $U_{DC}$	300 V
Moment of inertia $J$	0.2 kg·m <sup>2</sup>

The comparison between simulation and experiment is based on a non-linearity measure  $\Delta i_{nl}$  computed for the midpoint of each PWM cycle. The actual value of motor phase current is sampled at the midpoint of PWM cycle and compared with a theoretical value relying on a linear current changes assumption, i.e. with the average of instantaneous currents at the beginning and at the end of the cycle:

$$\Delta i_{nl} = (i_{t=0} + i_{t=T})/2 - i_{t=T/2} \quad (3)$$

As the rotor movement affects all the phase currents in a similar manner, the validation focuses on the A-phase, thus only  $\Delta i_{a-nl}$  measure is analyzed. The validation scenario consists of accelerating from standstill to the rated speed. The drive is forced to operate with maximal torque, hence the r.m.s. values of quasi-sine shaped phase currents are kept at the rated value of 10 A. The results were recorded for the reference model running both in fundamental component and PWM mode (Fig. 4 and Fig. 5, respectively), and for the laboratory drive (Fig. 6). The upper parts ('a') of the figures cover whole duration of the test, while the lower parts ('b') consist of a zoomed part corresponding to operating at rated speed.

The simulation outcomes show that the non-linearity measure changes in a quasi-sine manner and its amplitude is related to the rotor angular speed. At the maximal speed of 2200 rad/s, the amplitude of the non-linearity measure reaches 1.8 A. The outcomes of both variants of simulation are identical.

The experimental results, shown in Fig. 6, were recorded using the microprocessor-based controller. Due to limitation of the communication interface between the drive controller and the host computer the waveforms are composed from points recorded with a frequency of 2.5 kHz. The non-linearity measure appears to have higher peak values than in simulation, reaching 3.4 A; nevertheless, it is assumed to origin from measurement disturbances. As operating at high speed requires maintaining inverter output voltage near its limit, the passive inverter states are narrow [17]. Consequently, the current sampling, which takes place in the middle of the passive states, is carried out shortly after transistors' switching when the current disturbances are distinctive. Nevertheless, despite the disturbances, the phase co-relation between the non-linearity measure and the phase current waveforms, as well as the relation between the non-linearity error amplitude and the speed are consistent with the previously discussed simulation outcomes.

In order to diminish the impact of noise included in the experimental results and to compare the non-linearity measure at different speeds, the test results were postprocessed. Fast Fourier Transform was used to compute the amplitude  $\Delta I_{a-nl}$  of fundamental-frequency component of the non-linearity

measure. This amplitude was next divided by phase current amplitude  $I_a$  to obtain a relative value. The above-explained computations were carried out for different time intervals of the drive acceleration process, which allowed for presenting the relative non-linearity measure  $\Delta I_{a-nl}/\Delta I_a$  as a function of rotor speed  $\omega$  (Fig. 7). Identical graphs were obtained for simulations reflecting fundamental component and PWM. The trend of experimental results confirms the correctness of the simulation.

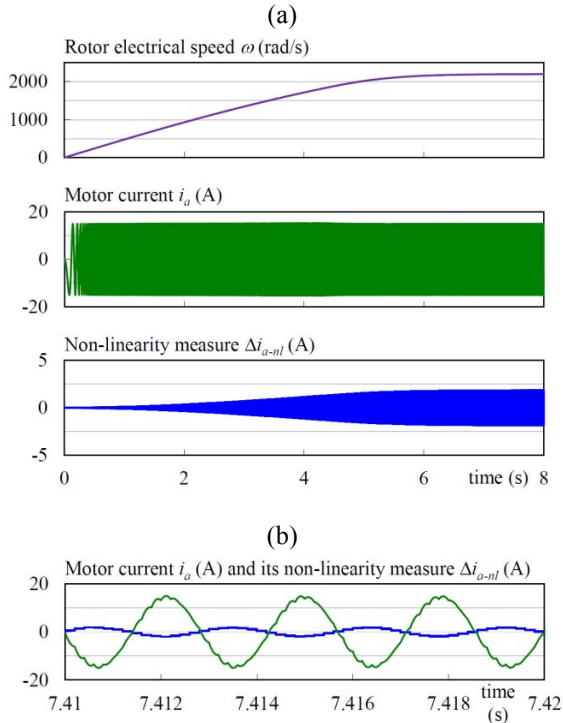


Fig. 4: Results from the reference model running in fundamental components mode: in (a) seconds and (b) milliseconds timescale

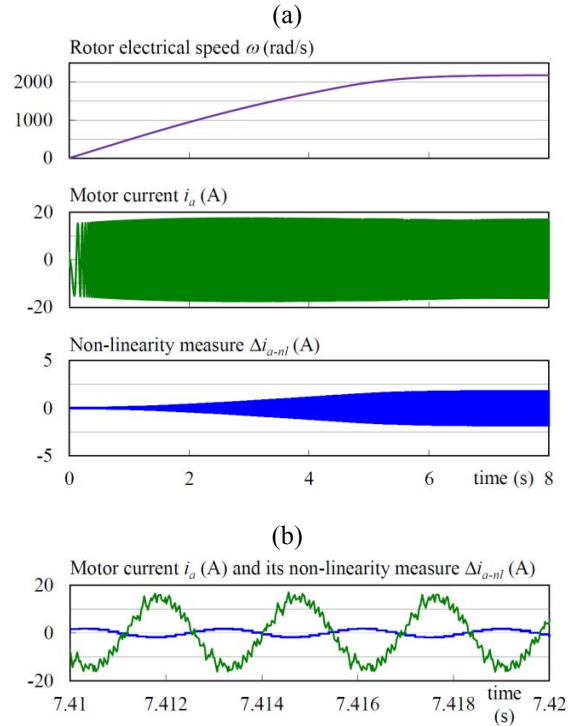


Fig. 5: Results from the reference model running in PWM mode: in (a) seconds and (b) milliseconds timescale

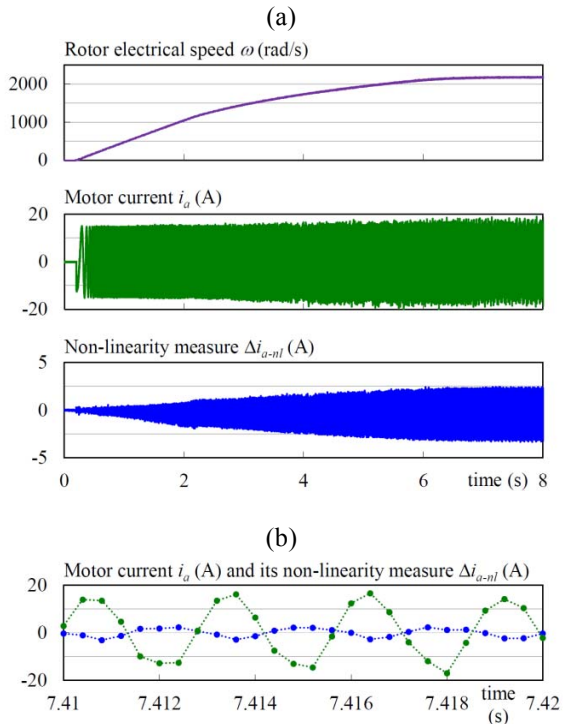


Fig. 6: Results from the laboratory drive: in (a) seconds and (b) milliseconds timescale

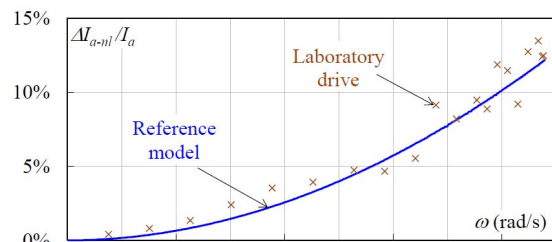


Fig. 7: The relative non-linearity measure as a function of rotor speed

## Conclusion

The proposed reference model enables analyzing motor currents waveforms including the non-linearity related to rotor progressive motion. The model does not reflect current disturbances associated to parasitic capacities, which cause the differences between simulation and experimental outcomes. Nevertheless, such level of details would make the model specific for a particular application. The proposed reference model represents general features, which is desirable when using it for developing universal current measurement algorithms.

The discrete operation of the controller and inverter was modeled by the use of triggered subsystems. Such approach is very transparent and fast executed. Moreover, it does not require using any specific toolboxes.

As the outcomes obtained using both variants of simulation are the same, it is concluded that the considered phenomena can be well represented in the fundamental components approach. Future work is aimed at developing a simplified mathematical model that will be able to reproduce the current non-linear changes based solely on input variables that are measurable by a typical microprocessor-based drive controller. This, in turn, will allow for proposing improved current measurement and prediction algorithms dedicated for high-speed drives.

## References

- [1] T. Matsui, T. Okuyama, J. Takahashi, T. Sukegawa, and K. Kamiyama, "A high accuracy current component detection method for fully digital vector-controlled PWM VSI-fed AC drives," *IEEE Transactions on Power Electronics*, vol. 5, no. 1, pp. 62–68, 1990.
- [2] S.-H. Song, J.-W. Choi, and S.-K. Sul, "Current measurements in digitally controlled AC drives," *Industry Applications Magazine, IEEE*, vol. 6, no. 4, pp. 51–62, 2000.
- [3] J. Böcker and O. Buchholz, "Can oversampling improve the dynamics of PWM controls?," in *Industrial Technology (ICIT), 2013 IEEE International Conference on*, 2013, pp. 1818–1824.
- [4] C. K. Lin, J. t Yu, Y. S. Lai, H. C. Yu, Y. H. Lin, and F. M. Chen, "Simplified model-free predictive current control for interior permanent magnet synchronous motors," *Electronics Letters*, vol. 52, no. 1, pp. 49–50, 2016.
- [5] L. Jarzebowicz, A. Opalinski, and M. Cisek, "Improving Control Dynamics of PMSM Drive by Estimating Zero-Delay Current Value," *Elektronika ir Elektrotechnika*, vol. 21, no. 2, Apr. 2015.
- [6] A. Anuchin and V. Kozachenko, "Current loop dead-beat control with the digital PI-controller," in *2014 16th European Conference on Power Electronics and Applications (EPE'14-ECCE Europe)*, 2014, pp. 1–8.
- [7] C. M. Wolf, M. W. Degner, and F. Briz, "Analysis of current sampling errors in PWM, VSI drives," in *Energy Conversion Congress and Exposition (ECCE), 2013 IEEE*, 2013, pp. 1770–1777.
- [8] L. Jarzebowicz, "Errors of a linear current approximation in high speed PMSM drives," *IEEE Transactions on Power Electronics*, vol. PP, no. 99, pp. 1–1, 2017. DOI: 10.1109/TPEL.2017.2694450.
- [9] D. Adameczyk, A. Wilk, and M. Michna, "Model of the double-rotor induction motor in terms of electromagnetic differential," *Archives of Electrical Engineering*, vol. 65, no. 4, pp. 761–772, 2016.
- [10] K. H. Nam, *AC Motor Control and Electrical Vehicle Applications*. CRC Press, 2010.
- [11] S. K. Sahoo and T. Bhattacharya, "Rotor Flux-Oriented Control of Induction Motor With Synchronized Sinusoidal PWM for Traction Application," *IEEE Transactions on Power Electronics*, vol. 31, no. 6, pp. 4429–4439, Jun. 2016.
- [12] Y.-C. Kwon, S. Kim, and S.-K. Sul, "Six-Step Operation of PMSM With Instantaneous Current Control," *IEEE Transactions on Industry Applications*, vol. 50, no. 4, pp. 2614–2625, Jul. 2014.
- [13] T. Sun, C. Liu, N. Lu, D. Gao, and S. Xu, "Design of PMSM vector control system based on TMS320F2812 DSP," in *Power Electronics and Motion Control Conference (IPEMC), 2012 7th International*, 2012, vol. 4, pp. 2602–2606.

- [14] T. Tarczewski and L. M. Grzesiak, "Constrained State Feedback Speed Control of PMSM Based on Model Predictive Approach," *IEEE Transactions on Industrial Electronics*, vol. 63, no. 6, pp. 3867–3875, Jun. 2016.
- [15] F. Wilczyński, M. Morawiec, P. Strankowski, J. Guziński, and A. Lewicki, "Sensorless field oriented control of five phase induction motor with third harmonic injection," in *2017 11th IEEE International Conference on Compatibility, Power Electronics and Power Engineering (CPE-POWERENG)*, 2017, pp. 392–397.
- [16] S. De Pablo, A. B. Rey, L. C. Herrero, and J. M. Ruiz, "A simpler and faster method for SVM implementation," in *2007 European Conference on Power Electronics and Applications*, 2007, pp. 1–9.
- [17] S. Bolognani, S. Calligaro, R. Petrella, and M. Sterpellone, "Sensorless control for IPMSM using PWM excitation: Analytical developments and implementation issues," in *Sensorless Control for Electrical Drives (SLED), 2011 Symposium on*, 2011, pp. 64–73.